

Novel Metallacycles via Nucleophilic Aminomethylation: 5,5-Bis(cyclopentadienyl)-1,3-diaza-5-zirconacyclohexane and Related Organometallic Heterocycles

Hans H. Karsch,* Kai-A. Schreiber, and Manfred Reisky

Anorganisch-Chemisches Institut der Technischen Universität München, Lichtenbergstrasse 4, D-85747 Garching, Germany

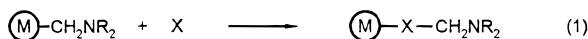
Received June 8, 1998

The doubly lithiated aminals bis(lithiomethyl(methylamino))methane [LiCH₂N(Me)]₂CH₂ (**1a**) and bis(lithiomethyl-isopropylamino)methane [LiCH₂N(*i*-Pr)]₂CH₂ (**1b**) react with Cp- and Cp*- (Cp* = C₅Me₅) substituted zirconocene chlorides in toluene to give Cp₂ZrCH₂N-(R)CH₂N(R)CH₂ (**2a**, R = Me; **2c**, R = *i*-Pr) and Cp*₂ZrCH₂N(R)CH₂N(R)CH₂ (**2b**, R = Me; **2d**, R = *i*-Pr). An interaction of the nitrogen atoms of the metallacycles with the zirconium centers in the solid state (**2a**, **2b**) and in solution (**2a**, **2c**) is deduced from structural studies and from the ¹H NMR spectra at variable temperatures (Δ*G*[‡] = 65.7 ± 0.6 kJ mol⁻¹ for the ring inversion process in **2c**). Isonitriles CNR (R = *t*-Bu, Me) and CO insert in one of the zirconium methylene σ-bonds of **2b** and **2d** and yield Cp*₂Zr[N(R²)CCH₂N(R¹)CH₂N(R¹)-CH₂] (**3a**, R¹ = Me, R² = *t*-Bu; **3b**, R¹ = *i*-Pr, R² = *t*-Bu; **3c**, R¹, R² = Me) and the zirconium enolates Cp*₂Zr(H)[OC=CHN(R)CH₂N(R)CH₂] (**4a**, R = Me; **4b**, R = *i*-Pr), respectively. Further insertion of isocyanides does not occur. Complexes **2a** and **2c** are unaffected by isocyanides or CO. The molecular structures of **2a**, **2b**, and **3a** have been studied by X-ray diffraction. The resulting structural information of the complexes **2a** and **2b** provides valuable insight into the nature of the Zr ← N interaction within the metallacycles, which is discussed briefly.

Introduction

Aminomethyl functionalities at transition metal centers in principle would provide a plethora of useful aspects for organic synthesis.

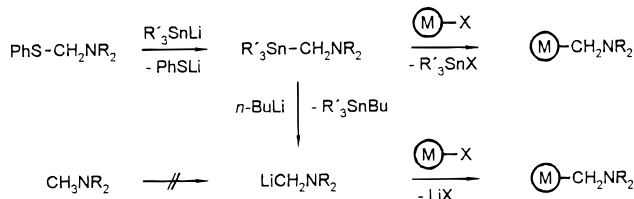
In particular, insertion reactions (eq 1) of CO, CO₂, or homologues would give access to a multitude of amino acid derivatives.



(M) = fragment of transition metal complex
(X = CO, CO₂, CNR, C(NR₂)₂ ...)

The general method in organometallic chemistry for the generation of a metal–alkyl bond is a nucleophilic alkylation (usually by means of alkyllithium or Grignard reagents), but direct metalation of methylamines is difficult to achieve. In fact, there is no example of direct lithiation of methylamines and subsequent use for transmetalation with transition metal centers. Only by using the organotin route, either directly¹ or via transformation to the aminomethyl lithium derivative²

Scheme 1



have some rare examples of aminomethyl-substituted transition metal complexes been obtained (Scheme 1).^{3,4}

Some reactivity studies at zirconocene metal centers confirm the potential of these compounds for organic synthesis, but the investigations obviously are hampered by the restricted synthetic access for the starting complexes.^{3c} Therefore an easy access to aminomethyl transition metal complexes would be highly desirable.

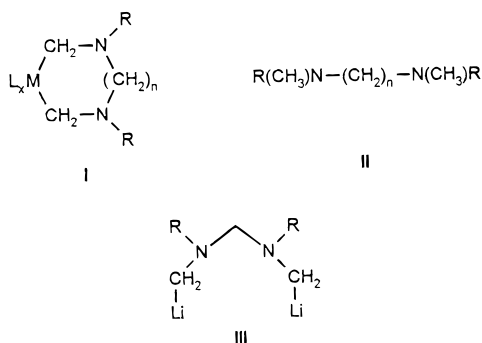
Double lithiated difunctional methylamines and, hence, metalaazaheterocycles **I** (Figure 1) would even be of

(2) (a) Peterson, D. J. *J. Organomet. Chem.* **1970**, *21*, P63. (b) Peterson, D. J. *J. Am. Chem. Soc.* **1971**, *93*, 4027. (c) Quintard, J.-P.; Elissondo, B.; Jousseau, B. *Synthesis* **1984**, 495. (d) Peterson, D. J.; Ward, J. T. *J. Organomet. Chem.* **1974**, *66*, 209.

(3) (a) Lubben, T. V.; Ploessl, K.; Norton, J. R.; Miller, M. M.; Anderson, O. P. *Organometallics* **1992**, *11*, 122–127. (b) Ploessl, K.; Norton, J. R. *Organometallics* **1992**, *11*, 534–539. (c) Gately, D. A.; Norton, J. R.; Goodson, P. A. *J. Am. Chem. Soc.* **1995**, *117*, 986–996.

(4) (a) Steinborn, D. Z. *Chem.* **1976**, *16*, 328. (b) Steinborn, D. Z. *Chem.* **1977**, *17*, 347.

(1) (a) Abel, E. W.; Rowley, R. J. *J. Chem. Soc., Dalton Trans.* **1975**, 1096. (b) Fong, C. W.; Wilkinson, G. *J. Chem. Soc., Dalton Trans.* **1975**, 1100.

**Figure 1.**

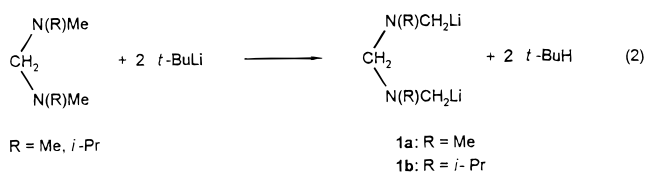
greater interest due to their increased functionality and presumably higher stability. However, complexes of this type are completely unknown.

Methyl-substituted diamines would be suitable precursors. Indeed, TMEDA (**II**; R = Me, $n = 2$) is metalated with *t*-BuLi under ambient conditions, but in a nonselective way, and transition metal derivatives have not been reported.⁵

Metalation of aminals (**II**; R = Me, $n = 1$) with *t*-BuLi likewise has been reported to produce an insoluble white precipitate, which has not been investigated further.⁶ We have investigated the lithiation of **II** (R = Me, *i*-Pr, Cy; $n = 1$) and found that double metalation to give **III** (R = Me, *i*-Pr, Cy; $n = 1$) occurs in good yield. Subsequently it could be demonstrated that these compounds can be used for nucleophilic aminomethylation reactions at main group centers (Si, Ge, Sn, P).⁷ Since aminals themselves are useful reagents in organic synthesis,⁸ transition metal heterocycles with a cyclic aminal backbone **I** ($n = 1$) might provide an interesting synthetic potential.

Results and Discussion

1. Synthesis, Structure, and Spectroscopy of 2a–d. Lithiation of methyl aminals R(Me)NCH₂N(Me)R according to eq 2 gave pyrophoric, almost insoluble white powders **1a,b** from pentane.⁷



Double metalation at two *N*-methyl groups was deduced from a variety of derivatives, obtained from subsequent reactions of **1a,b**,⁷ but NMR spectra were not obtained at this stage. We now found that by using coordinating solvent mixtures PMDETA/THF or TMEDA/THF the solubility of **1a,b** is enhanced to an extent that

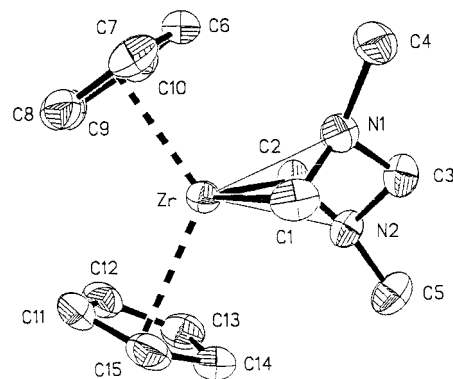


Figure 2. Molecular structure of Cp₂ZrCH₂N(Me)CH₂N(Me)CH₂ (**2a**) drawn with 50% probability ellipsoids. Selected bond lengths (Å): Zr–C(1) 2.263(3); Zr–C(2) 2.280(3); Zr–N(1) 2.423(2); Zr–N(2) 2.455(2); Zr–X1A 2.293; Zr–X1B 2.286; C(1)–N(1) 1.466(4); C(2)–N(2) 1.483(4). Selected bond angles (deg): N(1)–C(3)–N(2) 105.2(2); C(1)–Zr–C(2) 104.5(1); X1A–Zr–X1B 122.0; N(1)–C(1)–Zr 77.8(2); N(2)–C(2)–Zr 78.3(2); C(1)–N(1)–Zr 65.9(2); C(2)–N(2)–Zr 65.4(1).

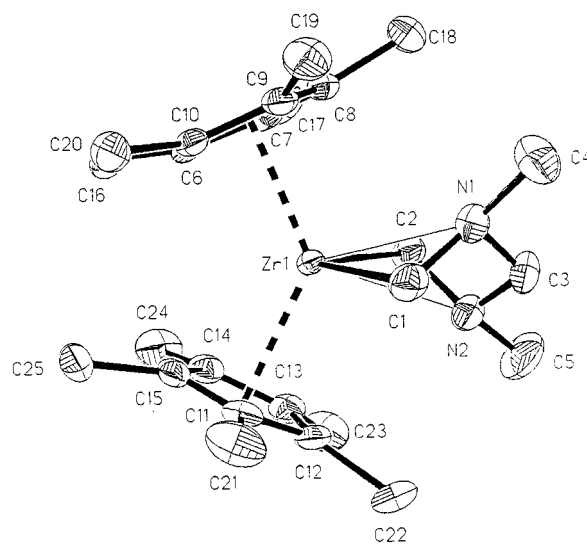


Figure 3. Molecular structure of Cp*₂ZrCH₂N(Me)CH₂N(Me)CH₂ (**2b**) drawn with 50% probability ellipsoids. Selected bond lengths (Å): Zr–C(1) 2.260(3); Zr–C(2) 2.288(3); Zr–N(1) 2.593(2); Zr–N(2) 2.720(2); Zr–X1A 2.312; Zr–X1B 2.315; C(1)–N(1) 1.476(4); C(2)–N(2) 1.470(4). Selected bond angles (deg): N(1)–C(3)–N(2) 111.7(2); C(1)–Zr–C(2) 100.2(1); X1A–Zr–X1B 131.5; N(1)–C(1)–Zr 85.2(2); N(2)–C(2)–Zr 90.0(2); C(1)–N(1)–Zr 60.3(1); C(2)–N(2)–Zr 57.3(1).

NMR spectra can be recorded. Thus, a 1:1 mixture of **1a** and PMDETA in THF displays an AB pattern in the ¹H NMR spectrum for the lithium methylene protons (δ NCH₂Li = 0.54/0.93, ²J_{H–H} = 12.1 Hz) at 25 °C, which coalesce at +80 °C (δ NCH₂Li = 0.74). This coalescence indicates reversible lithium coordination (Li–C and Li–N) of the deprotonated aminal, presumably forming a three-membered ring ($\Delta G^\ddagger = 62.09 \pm 0.4$ kJ mol^{–1}). Similarly, the ¹H NMR spectrum of a 1:1 mixture of **1a** and TMEDA in THF displays an AB pattern for the lithium methylene protons (δ NCH₂Li = 0.45/0.87, ²J_{H–H} = 12.1 Hz) at 25 °C. Coalescence is observed at +60

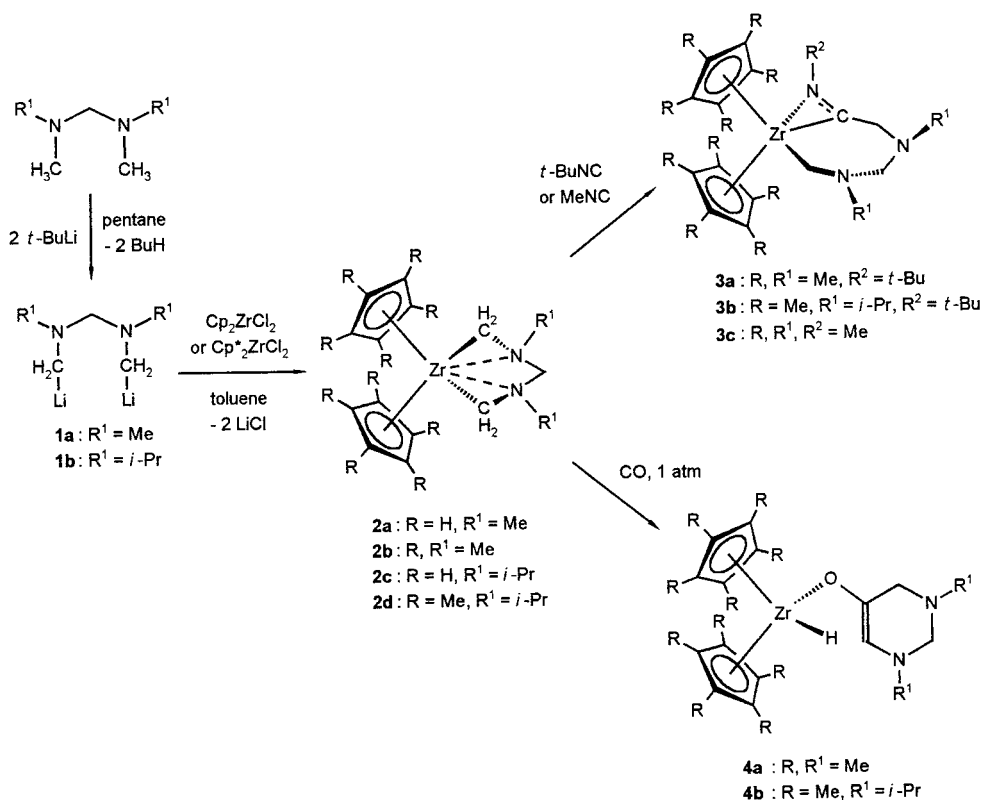
(5) (a) Langer, A. W., Jr. *N. Y. Acad. Sci.* **1965**, *27*, 741. (b) Köhler, F. H.; Hertkorn, N.; Blümel, J. *Chem. Ber./Rec.* **1987**, *120*, 2081. (c) Harder, S.; Lutz, M. *Organometallics* **1994**, *13*, 5173.

(6) Smith, N. N. *Adv. Chem. Ser.* **1974**, *130*, 23.

(7) (a) Karsch, H. H. *Chem. Ber.* **1996**, *129*, 483. (b) Karsch, H. H.; Schreiber, K.-A.; Herker, M. *Chem. Ber./Rec.* **1997**, *130*, 1777–1785.

(8) (a) Duhamel, L. *The Chemistry of Functional Groups; Supplement F. The Chemistry of Amino, Nitroso, and Nitro Compounds and Their Derivatives*; Patai, S., Ed.; J. Wiley & Sons: New York, 1982; pp 849–907. (b) Böhme, H.; Viehe, H. G. In *Iminium Salts in Organic Chemistry*; Böhme, H., Ed.; *Advances in Organic Chemistry*, Vol. 9; Taylor, E. C., Ed.; J. Wiley & Sons: New York, 1976; p 120ff.

Scheme 2



$^\circ\text{C}$ ($\delta \text{NCH}_2\text{Li} = 0.68$). In both cases, colorless crystals could be obtained from the solutions (see Experimental Section).

Whereas temperature-dependent ^1H NMR spectra of aminomethyl lithium compounds have not yet been reported, these results have to be compared to some structural findings: as yet, the structures of three aminomethyl lithium compounds have been reported and all three structures are quite different.^{9,10} However, (multiple bridging) C coordination in all three cases and nitrogen coordination in two cases (i.e., formation of a Li–C–N three-membered ring) are observed in the solid state. Both kinds of lithium coordination are likely to occur also in the present cases.

According to Scheme 2, compounds **2a–d** were obtained by reacting Cp_2ZrCl_2 or Cp^*ZrCl_2 with the doubly lithiated aminomethyl ligands **1a** or **1b** in toluene solution with satisfactory to high yields.

2a–2c were obtained as colorless; **2d** was obtained as red crystals. Crystals of **2a** and **2b** were suitable for X-ray analysis. Their structures are shown in Figures 2 and Figure 3.

In structures **2a** and **2b**, the six-membered zirconia-heterocycles adopt a twist conformation. Zr–C1 and Zr–C2 bond distances are similar to those in Cp_2ZrMe_2 (2.28/2.27 Å)¹¹ and slightly shorter than in the structurally characterized 18-electron aminomethyl zirconium complex $\text{Cp}_2(\text{TFA})\text{ZrCHPhNMe}_2$ (**IV**) (TFA = O_2CCF_3) ($d(\text{Zr}–\text{C}) = 2.30$ Å),^{3a} shown in Figure 4.

(9) Boche, G.; Marsch, M.; Harbach, J.; Harms, K.; Ledig, B.; Schubert, F.; Lohrenz, J. C. W.; Ahlbrecht, H. *Chem. Ber./Rec.* **1993**, *126*, 1887–1894.

(10) Becke, F.; Heinemann, F. W.; Rüffer, T.; Wiegeleben, P.; Boese, R.; Bläser, D.; Steinborn, D. *J. Organomet. Chem.* **1997**, *548*, 205–210.

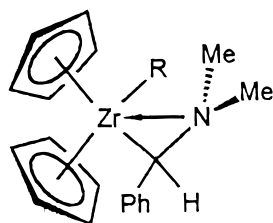
(11) Hunter, W. E.; Hrcncir, D. C.; Bynum, R. V.; Pentilla, R. A.; Atwood, J. L. *Organometallics* **1983**, *2*, 750–755.

The C–N bond lengths in both complexes are in the typical range for a C–N single-bond distance. The Zr–ring centroid distance in **2a** and in **2b** as well as the X1A–Zr–X1B angles in both compounds compare well with those of other Cp_2ZrR_2 and Cp^*ZrR_2 complexes.^{3a,11,12} In both structures, the C1 and C2 carbon atoms of the aminomethyl ligands are placed in a plane perpendicular to that of the normals to the metallocene rings in common with 16-electron compounds Cp_2ZrR_2 .¹¹ The C1–Zr–C2 angles decrease from **2a** to **2b** to Cp_2ZrMe_2 (95.6°).¹¹ The nitrogen atoms N1 and N2 lie above and below the plane C1ZrC2 (see Figure 5), the latter thus forming an interplanar angle ψ with the plane N1C3N2 (=plane N1ZrN2) of 44.5° (**2a**) and 41.1° (**2b**), respectively.

2a and **2b** are chiral. Only the rac-forms were present in the solid state in both cases.

The main difference between the two structures concerns the Zr–N distances. The bonds Zr–N in **2a** are elongated compared to the Zr–N bond in the structurally characterized compound **IV** (2.312 (3) Å),^{3a} but much shorter than the Zr–N bonds in **2b**. The difference in Zr–N bond lengths in **2a** and **IV** in part may be a consequence of the deviation of the nitrogen atoms from the ideal plane and in part due to the double nitrogen coordination in **2a**. Formally **2a** may be regarded as a 20-electron complex with two η^2 -bonded aminomethyl ligands. The electronically more saturated zirconium center and the steric demand of the Cp^* ligands clearly are responsible for the elongated Zr–N bond lengths in **2b**. The steric needs of the Cp^* ligands in **2b** are also reflected by the deviation of the methyl substituents from the C_5 plane (mean: 0.264°),

(12) Bortolin, R.; Patel, V.; Munday, I.; Taylor, N. J.; Carty, A. J. *J. Chem. Soc., Chem. Commun.* **1985**, 456.



IV : R = TFA

Figure 4.

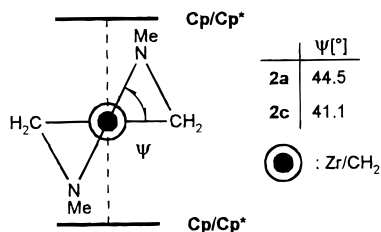


Figure 5.

in accordance with other complexes with a Cp*₂Zr unit.¹² The individual C–C_(ring) distances and the Zr–C_(ring) distances deviate only slightly from the mean values (1.412 and 2.606 Å, respectively). Quite remarkably, this is also true for **2a** (C–C_(ring) mean value 1.400 Å; Zr–C_(ring) mean value 2.584 Å). These deviations are much less than in other complexes, potentially violating the 18-electron rule, e.g., in Cp₄Zr.¹³

The ¹H NMR spectra of **2a** at –100 to +80 °C indicate equivalent N-donor atoms; the diastereotopic ZrCH₂N methylene protons at δ = 1.96 and 1.41 (²J_{H–H} = 8.9 Hz) verify that nitrogen remains coordinated in solution in the whole range. At room temperature, **2c** reveals a quite similar character (Figure 6): an AB pattern for the ZrCH₂N methylene protons (δ = 1.60, 1.90, ²J_{H–H} = 9.2 Hz) and two doublets (δ = 0.85, 0.93) for the diastereotopic methyl groups of the isopropyl substituents at +20 °C are observed. But at variance to **2a**, the AB pattern collapses to a broad single resonance (δ = 1.77) and the signal for the methyl groups to one single doublet (δ = 0.95) on heating the sample to +80 °C.

Therefore it seems reasonable to assume a weaker Zr–N bonding interaction for **2c** compared to **2a** as a consequence of a reversible bond dissociation (Zr–N) in **2c** at higher temperatures (ΔG^\ddagger = 65.7 ± 0.6 kJ mol^{–1}),¹⁴ probably due to steric effects. No significant temperature dependence was observed in the NMR spectra of **2b**. The ¹H NMR resonances of the ZrCH₂N and NCH₃ protons showed one single line from –100 to +80 °C. In line with the solid-state structure, the Zr–N bond of **2b** obviously is quite weak, and dissociation thus is facile in solution.

For **2d** one single doublet was observed for the isopropyl methyl groups (δ = 1.14) in the ¹H NMR spectrum and, as in **2b**, one singlet for the ZrCH₂N protons (δ = 1.07). Again, no temperature dependency was observed in the ¹H NMR spectra from –100 to +80 °C. Obviously, replacement of *N*-methyl groups as in

2b by isopropyl groups as in **2d** does not increase the nitrogen donor ability, and hence, a similar reaction behavior can be expected for **2b** and **2d**.

In conclusion, from structural and spectroscopic studies it emerges that **2a–d** represent at least three quite different types of zirconaheterocycles, distinguished by a different reactivity pattern: **2a** is expected to be rather inert to insertion reactions due to the highly saturated zirconium center. **2b** and **2d** should allow insertion reactions quite easily, similar to, for example, Cp*₂ZrCH₂(CH₂)₂CH₂.¹⁵ **2c** probably is an intermediate case: low reactivity at low temperature but insertions being possible at elevated temperatures.

2. Insertion reactions of 2a–d. Migratory insertions of isocyanides and carbon monoxide into zirconium–carbon σ -bonds are among the most investigated reactions in organometallic chemistry and very useful in many stoichiometric and catalytic processes.¹⁶ Reactions of numerous dicyclopentadienyl zirconium alkyls with different alkyl isocyanides have enabled the isolation and characterization of a large number of η^2 -iminoacyl complexes.¹⁷ Several mechanistic and theoretical studies on this insertion reaction have also been reported,¹⁸ and the “inside” or “outside” coordination of the nitrogen atom in the iminoacyl ligands generated has been extensively studied.^{3a,17,18a,19,20a} Zirconaheterocycles have also been studied.¹⁵ In addition, insertion of carbon monoxide into zirconium organyl bonds has attracted much attention and was investigated in detail.^{20,21} On the basis of these studies, one of the nine relevant orbitals in zirconocene dialkyl complexes occupies the central equatorial position, mutually cis to both alkyl ligands. In our case, this is the orbital that interacts with the lone pairs of one or both nitrogen atoms of the metallacyclic aminal **2a–d**. Reactions of toluene solutions of the zirconium complexes **2b** and **2d** with 1 equiv of *t*-BuNC or MeNC at room temperature led to yellow (**3a**) or colorless (**3b**, **3c**) solids, which were identified as iminoacyl complexes Cp*₂Zr[N(R²)CCH₂N(R¹)CH₂N(R¹)CH₂] (**3a**, R¹ = Me, R² = *t*-Bu; **3b**, R¹ = *i*-Pr, R² = *t*-Bu; **3c**, R¹, R² = Me). Compounds **3a–c** did not react with further isocyanide even at +80 °C.

In contrast, complex **2a** was unaffected by treatment with *t*-BuNC or MeNC even at rather forcing reaction conditions (refluxing toluene). Addition of catalytic or even equimolar amounts of AlCl₃ or MgCl₂ likewise failed to promote an insertion reaction. A minor amount

(15) Manriquez, J. M.; McAllister D. R.; Sanner, R. D.; Bercaw, J. E. *J. Am. Chem. Soc.* **1978**, *100*, 2716.

(16) Durfee, L. D.; Rothwell, I. P. *Chem. Rev.* **1988**, *88*, 1059.

(17) Chamberlain, L. R.; Durfee, L. D.; Fanwick, P. E.; Kobriger, L. M.; Latesky, S. L.; McMullen, A. K.; Steffey, B. D.; Rothwell, I. P.; Folting, K.; Huffman, J. C.; Streib, W. E.; Wang, R. *J. Am. Chem. Soc.* **1987**, *109*, 390.

(18) (a) Campion, B. K.; Falk, J.; Tilley, T. D. *J. Am. Chem. Soc.* **1987**, *109*, 2049. (b) Lappert, M. F.; Luong-Thi, N. T.; Melne, C. R. C. *J. Organomet. Chem.* **1979**, *174*, C35.

(19) Barriola, A. M.; Cano, A. M.; Cuenca, T.; Fernandez, F. J.; Gomez-Sal, P.; Manzanero, A.; Royo, P. *J. Organomet. Chem.* **1997**, *542*, 247–253.

(20) (a) Erker, G.; Rosenfeldt, F. *J. Organomet. Chem.* **1980**, *188*, C1–C4. (b) Erker, G.; Rosenfeldt, F. *Angew. Chem.* **1978**, *90*, 640; *Angew. Chem., Int. Ed. Engl.* **1978**, *17*, 605. (c) Erker, G. *Acc. Chem. Res.* **1984**, *17*, 103.

(21) (a) Fachinetti, G.; Floriani, C.; Marchetti, F.; Merlino, S. *J. Chem. Soc., Chem. Commun.* **1976**, 522. (b) Fachinetti, G.; Fochi, G.; Floriani, C. *J. Chem. Soc., Dalton Trans.* **1977**, 1946–1949.

(13) Rogers, R. D.; Vann Bynum, R.; Atwood, J. L. *J. Am. Chem. Soc.* **1978**, *100*, 5238.

(14) Fribolin, H. *Basic One- and Two-Dimensional NMR Spectroscopy*; VCH: Weinheim, 1993; pp 293–296.

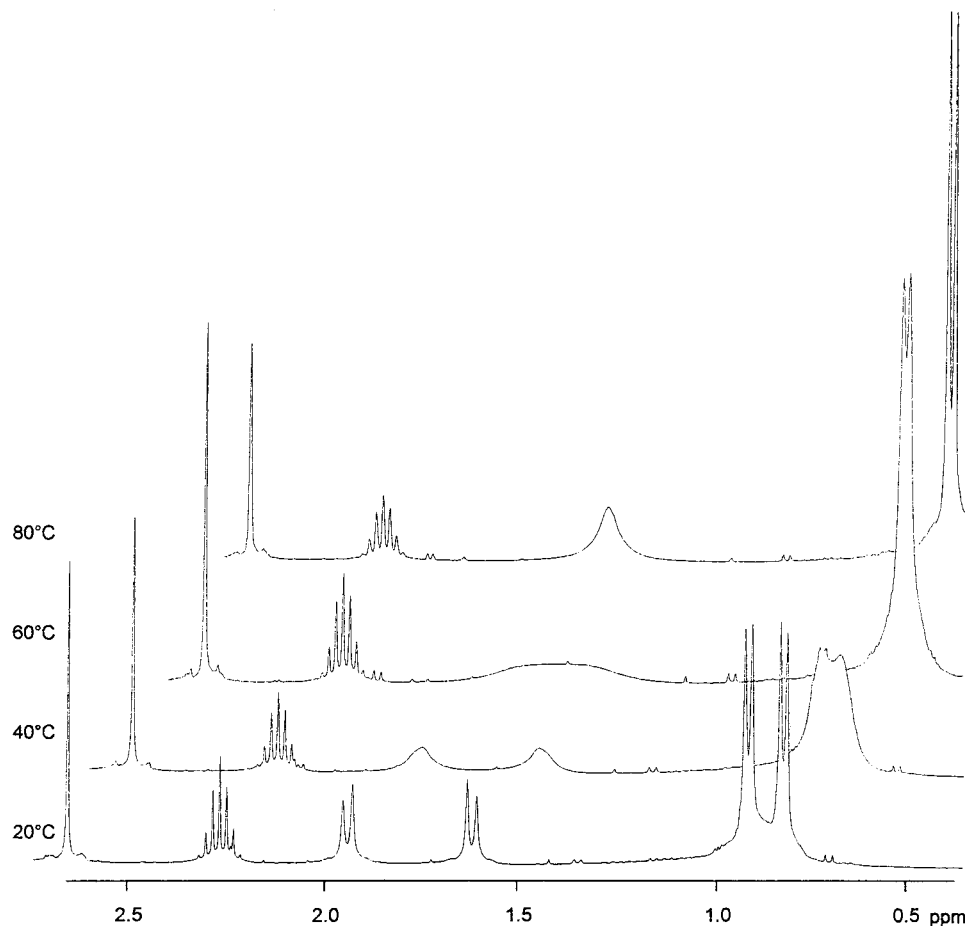


Figure 6. Temperature dependence of experimental line shapes for ZrCH₂N methylene and isopropyl proton resonances of Cp₂ZrCH₂N(*i*-Pr)CH₂N(*i*-Pr)CH₂ (**2c**) in C₆D₆ solution at 400 MHz.

of Cp₂ZrCl₂ but no remaining **2a** was detected in the decomposition product mixture in both cases. The mixture could not be identified further, however.

The ¹H NMR resonances for the Cp* methyl groups, the *tert*-butyl substituents, the iminoacyl methyl group, and the diaminomethylene bridges of **3a**, **3b**, and **3c** appear as singlets. For each compound (**3a–c**) three different singlet resonances are observed for the three methylene groups. The aminal *N*-methyl resonances of **3a** and **3c** appear as two distinguishable singlets in each spectrum; both *N*-isopropyl groups of **3b** are detected as two doublets. The assignment of the {¹H}¹³C NMR resonances of **3a** and **3b** has been checked by proton-coupled ¹³C NMR spectra. An odd numbered, symmetrical multiplet of low intensity at δ 240.0 for **3a** and a singlet at δ 239.7 for **3b** are consistent with the presence of η²-iminoacyl fragments in **3a** and **3b**.^{18b,19,22} The ν(CN) stretching mode is observed at 1618 cm⁻¹ for **3a** and at 1625 cm⁻¹ for **3c**. Literature values for similar compounds range from 1490 to 1760 cm⁻¹.^{23–25}

Crystals of compound **3a** suitable for X-ray diffraction studies were obtained from pentane. Figure 7 shows the molecular structure of **3a** including the atom-labeling scheme.

The zirconabicyclic complex **3a** exhibits an “N-outside” conformation for the η²-iminoacyl fragment, which is bonded to the zirconium atom in an “edge-on” fashion. The insertion of *tert*-butyl isocyanide leads to the formation of two adjacent zirconacyclic rings of different size. The smaller three-membered ring containing Zr, C1, and N1 is characterized by an acute N1–Zr–C1 bond angle of 32.09 (9)° and a Zr–N1 bond of 2.343 (2) Å, which is noticeably longer than the Zr–C1 bond of 2.231 (2) Å. The C1–N1 bond is comparable to that found in other η²-iminoacyl complexes.^{19,22} The planes X1AZrX1B and C4ZrN1 are exactly orthogonal to each other, the iminoacyl carbon C1 is only 0.060 Å out of the C4ZrN1 plane, and the C4ZrN1/C1ZrN1 dihedral angle is 9.2°. No deflection from the Zr1N1C1 plane is observed for C5, according to the sum of angles around N1, which is exactly 360°. The atoms Zr1, C1, C2, C4, and N2 are almost coplanar with N1, whereas the atoms C3 and N3 are out of plane. The Zr–C4 (methylene) bond of 2.357 (3) Å is ca. 0.10 Å longer than the corresponding zirconium–carbon bond of 2.260 (3)

Å in the parent metallacycle Cp*₂ZrCH₂N(Me)CH₂N(Me)CH₂ (**2b**). This bond lengthening corresponds to

(22) Berg, F. J.; Petersen, J. L. *Organometallics* **1989**, *8*, 2461–2470.

(23) (a) den Haan, K. H.; Luinstra, G. A.; Meetsma, A.; Teuben, J. H. *Organometallics* **1987**, *6*, 1509. (b) Bochmann, M.; Wilson, L. M.; Hursthouse, M. B.; Short, R. L. *Organometallics* **1987**, *6*, 2556. (c) Erker, G.; Korek, U.; Petersen, J. L. *J. Organomet. Chem.* **1988**, *355*, 121.

(24) McMullen, A. K.; Rothwell, I. P.; Huffman, J. C. *J. Am. Chem. Soc.* **1985**, *107*, 1072.

(25) Bellachioma, G.; Cardaci, G.; Zanazzi, P. *Inorg. Chem.* **1987**, *26*, 84.

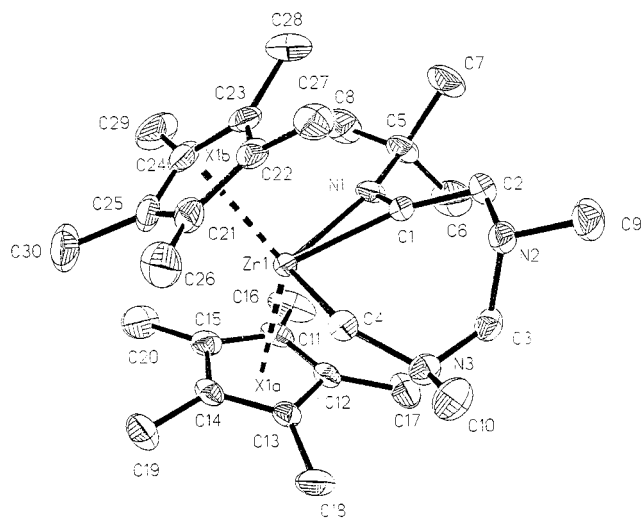


Figure 7. Molecular structure of $\text{Cp}^*_2\text{Zr}[\text{N}(\text{CMe}_3)\text{CCH}_2\text{N}(\text{Me})\text{CH}_2\text{N}(\text{Me})\text{CH}_2\text{N}(\text{Me})\text{CH}_2]$ (**3a**) drawn with 50% probability ellipsoids. Selected bond lengths (Å): Zr–C(1) 2.231(2); Zr–C(4) 2.357(3); Zr–N(1) 2.343(2); C(1)–C(2) 1.497(4); Zr–X1A 2.324; Zr–X1B 2.309; C(1)–N(1) 1.269(3); N(1)–C(5) 1.518(3). Selected bond angles (deg): C(1)–Zr–C(4) 81.30(9); C(1)–Zr–N(1) 32.09(9); N(1)–C(1)–C(2) 131.2(2); N(1)–C(1)–Zr 78.8(2); C(1)–N(1)–C(5) 128.4(2); X1A–Zr–X1B 133.7; Zr–N(1)–C(1) 69.1; C(2)–N(2)–C(3) 109.9(2); C(3)–N(3)–C(4) 114.7(2); Zr–C(1)–C(2) 150.0(2); C(1)–C(2)–N(2) 109.9(2); N(2)–C(3)–N(3) 116.5(2); N(3)–C(4)–Zr 126.0(2).

similar observations and has been attributed to the η^2 coordination mode of an iminoacyl fragment.²⁶ This interaction reduces the acceptor ability of the remaining metal orbital and leads to an elongation of the second zirconium–carbon bond. The steric needs of the Cp^* ligands in **3a** are reflected by a 0.279 Å deviation of the methyl substituents from the C_5 plane for C16–C20 and 0.230 Å for C26–C30.

According to Scheme 2, reaction of **2b** or **2d** with CO at 20 °C in toluene occurs spontaneously, as judged from a rapid color change (see Experimental Section) and afforded predominantly the zirconocene hexenolate $\text{Cp}^*_2\text{Zr}(\text{H})(\text{OC}=\text{CHN}(\text{R})\text{CH}_2\text{N}(\text{R})\text{CH}_2)$ (**4a**, R = Me; **4b**, R = *i*-Pr). Minor amounts (ca. 5%) of products resulting from hydrolysis were detected in both cases as well. However, the complexes **2a** and **2c** are unaffected by CO under the same conditions.

Characteristic features of the ^1H NMR spectrum of **4a** are a singlet at δ 5.95 (1H, Zr–H), as well as a diagnostic triplet at δ 5.35 (1H, $^4J_{\text{H-H}} = 1.2$ Hz), and a doublet at δ 2.97 (2H, $^4J_{\text{H-H}} = 1.2$ Hz) for the vinylic and the methylene (NCH_2CO) hydrogens, respectively. The formation of the hexenolates **4a** and **4b** can be rationalized as outlined in Scheme 3, which is analogous to a reaction pathway proposed for the reaction of $\text{Cp}^*_2\text{ZrCH}_2(\text{CH}_2)_2\text{CH}_2$ with CO.¹⁵

Conclusion

Dimetalated aminals may form metallacycles with additional intramolecular metal–nitrogen interactions.

The latter are dependent on (and tunable by) the electronic needs of the metal center and determine the extent of reactivity. Particularly useful in this respect are zirconocene-based metallacycles, which were obtained from dimetalated aminals and the respective zirconocene dichlorides. It could be demonstrated that insertion reactions of isonitriles and carbon monoxide into one of the Zr–C σ -bonds of the metallacycles formed this way are feasible if bulky and electron-donating ligands (C_5Me_5) are coordinated to the metal center (**2b**, **2d**). This is due to a weaker coordination of the aminal nitrogen atoms, whereas **2a** and **2c** with less electron donating Cp ligands are unaffected by these substrates. Studies on further reactions as well as an extension to other metal centers are in progress.

Experimental Section

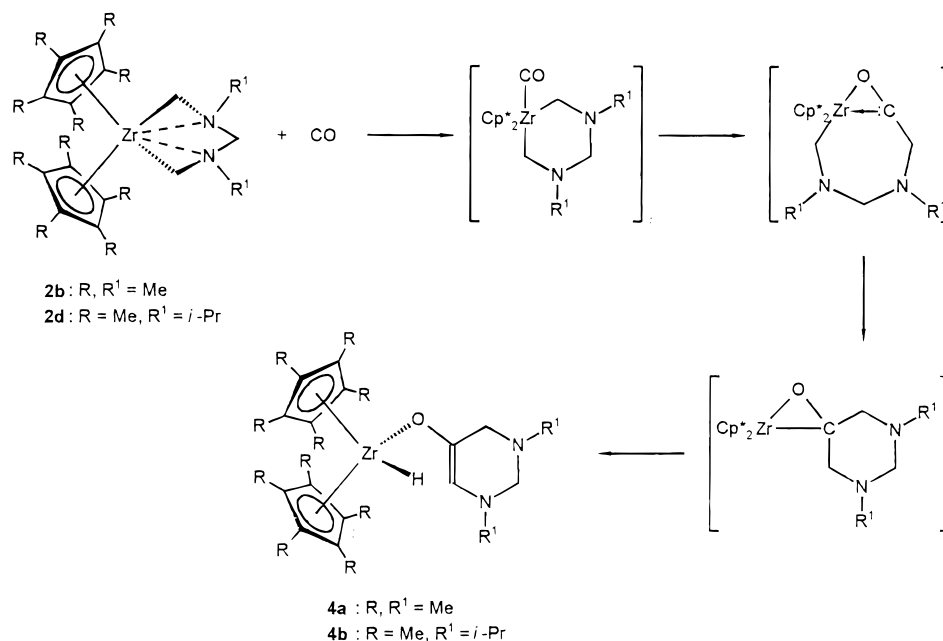
General Considerations. All operations were performed under a dry nitrogen atmosphere and with thoroughly dried glassware. Pentane, diethyl ether, toluene, and THF were distilled under N_2 from sodium/potassium alloy. Standard high-vacuum-line techniques were used. $\text{Cp}^*_2\text{ZrCl}_2$ ²⁷ ($\text{Cp}^* = \text{C}_5\text{Me}_5$) and solvent-free $[\text{LiCH}_2\text{N}(\text{R})_2\text{CH}_2]$ (R = Me, *i*-Pr)⁷ were synthesized according to literature procedures. *t*-BuLi (pentane solution 15%) was a donation of the Metallgesellschaft and was used as received. All other reagents were from commercial sources and used without further purification.

The elemental analyses were performed by Microanalytisches Labor der TU Muenchen. Chemical ionization (CI) mass spectra were obtained with a Varian MAT 311A spectrometer. The ^1H and ^{13}C NMR data were collected on a JEOL GX 270 (270.05 MHz ^1H , 67.94 MHz ^{13}C) and a JEOL GX 400 spectrometer (399.65 MHz ^1H , 100.40 MHz ^{13}C). ^1H and ^{13}C NMR chemical shifts (δ) are referenced to the internal residual proton or natural abundance ^{13}C resonances of the deuterated solvent relative to TMS ($\delta = 0$). The ^7Li NMR data were collected on a JEOL JNM Lambda 400 (155.40 MHz ^7Li). The chemical shifts ($\delta(^7\text{Li})$) are reported relative to a solution of LiCl (20%) in D_2O (external). All measurements were carried out at 25 °C in C_6D_6 . Exceptions are given separately. All chemical shifts are reported in parts per million (ppm) and coupling constants *J* in hertz. IR data were collected on a Nicolet 5DX FT-IR spectrophotometer.

Preparation of $2[\text{LiCH}_2\text{N}(\text{Me})_2\text{CH}_2 \times 2\text{THF} \times \text{PMDETA}]$. To a stirred suspension of freshly isolated bis(lithiomethyl(methylamino)methane $\{[\text{LiCH}_2\text{N}(\text{Me})_2\text{CH}_2]\}$ (**1a**) (0.58 g, 5.09 mmol) in 40 mL of pentane was added pentamethyldiethylenetriamine (PMDETA) (2.66 mL, 2.20 mmol) at -78 °C while stirring. The mixture was gradually warmed to room temperature (25 °C) and then stirred for a further 3 h. After 20 mL of THF was condensed into the reaction vessel at -78 °C, a clear solution resulted. The solution was concentrated and crystallization was carried out at -25 °C to give a colorless, crystalline product that consists of PMDETA, THF, and $[\text{LiCH}_2\text{N}(\text{Me})_2\text{CH}_2]$ (**1a**) in a 1:2:2 ratio. This ratio is unaffected by drying the crystals in vacuo. Yield: 0.70 g or 40%. CI-MS [*m/e* (%): 401 (2), [$\text{M}^+ - 2 \text{THF}$]; 387 (3), [401 – 2 Li]; 245 (21), [387 – $\text{Me}_2\text{N}(\text{CH}_2)_2\text{N}(\text{Me})\text{CH}_2\text{CHN}$]; 174 (100), [PMDETA + H^+], 115 (89), [$[\text{LiCH}_2\text{N}(\text{CH}_3)_2\text{CH}_2 + \text{H}^+]$]. ^1H NMR (dioxane- d_6 , 60 °C, 270.05 MHz): δ 0.74 (s br, 8 H, $\text{NCH}_2\text{-Li}$), 1.77 [m, 8 H, CH_2 (THF)], 2.15 [s, 12 H, NCH_3 (PMDETA)], 2.19 (s br, 12 H, NCH_3), 2.20 [s, 3 H, NCH_3 (PMDETA)], 2.37 (s br, 4 H, NCH_2N), 2.41 [m, 8 H, CH_2CH_2 (PMDETA)], 3.61 [m, 8 H, CH_2O (THF)]. $\{^1\text{H}\}^{13}\text{C}$ NMR (THF- d_6 , 25 °C, 67.94 MHz): δ 26.4 [s, CH_2 (THF)], 43.4 [s, NCH_3 (PMDETA)], 46.3 [s, NCH_3 (PMDETA)], 53.7 (m br, NCH_2Li) 54.3 (s br, NCH_3), 58.9/57.4 [s, CH_2CH_2 (PMDETA)], 68.2 [s, CH_2O (THF)], 90.1 (s, NCH_2N). ^7Li NMR (THF- d_6 , 25 °C, 155.40 MHz): 3.8 (s).

(26) Lauher, J. W.; Hoffmann, R. *J. Am. Chem. Soc.* **1976**, *98*, 1729.

Scheme 3



Preparation of $[\text{LiCH}_2\text{N}(\text{Me})_2]\text{CH}_2 \times \text{THF}$ in the Presence of TMEDA. The reaction procedure and workup of the reaction was the same as described for the synthesis of the PMDETA adduct: 0.49 g (4.30 mmol) of **1a** and 30 mL of pentane were used; 1.00 mL (8.60 mmol) of TMEDA and 20 mL of THF were added to the suspension. Colorless crystals of $[\text{LiCH}_2\text{N}(\text{Me})_2]\text{CH}_2 \times \text{THF}$ (1:1) were obtained at -25°C . Yield: 0.39 g or 49%. The crystals obtained were dried in vacuo and characterized by mass and NMR spectroscopy. CI-MS [*m/e* (%): 102 (2), $[\text{Me}_2\text{NCH}_2\text{NMe}_2]^+$; 76 (100), $[\text{THF}]^+$. ^1H NMR (dioxane-*d*₆, 25°C , 270.05 MHz): δ 0.45 (d, 2 H, NCH_2Li , $^2J = 12.1$ Hz), 0.87 (d, 2 H, NCH_2Li , $^2J = 12.1$ Hz), 1.77 [m, 4 H, 4 CH_2 (THF)], 2.18 (s br, 6 H, NCH_3), 2.36 (s br, 2 H, NCH_2N), 3.62 [m, 4 H, CH_2O (THF)]. $\{^1\text{H}\}^{13}\text{C}$ NMR (dioxane-*d*₆, 25°C , 67.94 MHz): δ 26.2 [s, CH_2 (THF)], 54.3 (s br, NCH_3), 54.6 (m br, NCH_2Li), 68.0 [s, CH_2O (THF)], 89.7 (s, NCH_2N). ^7Li NMR (dioxane-*d*₆, 25°C , 155.40 MHz): 1.8 (s). Though the crystals do not contain TMEDA, the crystalline compound was not obtained from THF solutions without added TMEDA.

Preparation of $\text{Cp}^*_2\text{ZrCH}_2\text{N}(\text{Me})\text{CH}_2\text{N}(\text{Me})\text{CH}_2$ (2a**).** To a stirred solution of bis(lithiomethyl(methylamino)methane $\{[\text{LiCH}_2\text{N}(\text{Me})_2]\text{CH}_2\}$ (**1a**) (1.40 g, 12.28 mmol) in 30 mL of toluene was added a toluene slurry of $\text{Cp}^*_2\text{ZrCl}_2$ (3.59 g, 12.28 mmol) at -78°C . The mixture was gradually warmed to room temperature (25°C) and then stirred for a further 16 h at 60°C . The solvent was evaporated under reduced pressure. The residue was extracted twice with pentane (30 mL). After the solution was concentrated, crystallization was carried out at 0°C to give **2a** as colorless crystals. Yield: 2.01 g or 51%, dec $145\text{--}150^\circ\text{C}$. CI-MS [*m/e* (%): 320 (67), $[\text{M}^+ - \text{H}]$; 277 (55), $[\text{M}^+ - \text{CH}_2\text{NCH}_3]$; 262 (34), $[\text{M}^+ - \text{CH}_2\text{N}(\text{CH}_3)\text{CH}_2]$; 234 (29), $[\text{M}^+ - \text{CH}_2\text{NCH}_3]$; 220 (100), $[\text{Cp}^*_2\text{Zr}]^+$. ^1H NMR (C_6D_6 , 25°C , 399.65 MHz): δ 1.38 (d, $^2J = 8.8$ Hz, 2 H, NCH_2Zr), 1.86 (s, 6 H, NCH_3), 1.93 (d, $^2J = 8.8$ Hz, 2 H, NCH_2Zr), 2.19 (s, 2 H, NCH_2N), 5.49 (s, 10 H, Cp). $\{^1\text{H}\}^{13}\text{C}$ NMR (C_6D_6 , 25°C , 67.94 MHz): δ 43.5 (s, NCH_3), 52.6 (s, NCH_2Zr), 82.6 (s, NCH_2N), 103.9 (s, Cp). Anal. Calcd for $\text{C}_{15}\text{H}_{22}\text{N}_2\text{Zr}$: C, 56.03; H, 6.90; N, 8.70; Zr, 28.37. Found: C, 55.90; H, 7.23; N, 8.53; Zr, 28.19.

X-ray Structural Solution and Refinement. The same general procedures were employed to collect the X-ray diffraction data for complexes **2a**, **2b**, and **3a**. Crystal data collection and refinement parameters are given in Table 1, while selected bond lengths and angles are presented in Figures 2, 3, and 7.

ORTEP diagrams showing the solid-state conformations of **2a**, **2b**, and **3a** can be found in Figures 2, 3, and 7, respectively.

Compounds 2a, 2b, and 3a. Suitable single crystals of **2a**, **2b** and **3a** were sealed into glass capillaries and used for measurement of precise cell constants and for intensity data collection. X-ray intensity data were recorded at -74°C on an Enraf-Nonius CAD4 diffractometer utilizing monochromated Mo $K\alpha$ radiation ($\lambda = 0.71073 \text{ \AA}$). During data collections, three standard reflections were measured periodically as a general check of crystal and instrument stability. No significant changes were observed. The structures were solved by direct methods (SHELXS-86)^{28a} and refined by full-matrix least-squares techniques against I^2 (SHELXL-93).^{28b} Diffraction intensities were corrected for Lp and absorption effects. The thermal motions of all non-hydrogen atoms were treated anisotropically. All hydrogen atoms were calculated in idealized positions, and their isotropic thermal parameters were tied to that of the adjacent carbon atom by a factor of 1.5. The structure of **2a** converged for 165 refined parameters to R1 (wR2) = 0.0299 (0.0849) for 2210 reflections with $F > 4\sigma(F)$. The structure of **2b** converged for 265 refined parameters to R1 (wR2) = 0.0340 (0.0975) for 4139 reflections with $F > 4\sigma(F)$. The structure of **3a** converged for 322 refined parameters to R1 (wR2) = 0.0297 (0.0731) for 4198 reflections with $F > 4\sigma(F)$. Further information may be obtained from the Fachinformationszentrum Karlsruhe, Gesellschaft für wissenschaftlich-technische Information mbH, D-76344 Eggenstein-Leopoldshafen, on quoting the depository numbers CSD- 406389, 408673, 408607, the names of the authors, and the full journal citation.

Preparation of $\text{Cp}^*_2\text{ZrCH}_2\text{N}(\text{Me})\text{CH}_2\text{N}(\text{Me})\text{CH}_2$ (2b**).** Bis(lithiomethyl(methylamino)methane $\{[\text{LiCH}_2\text{N}(\text{Me})_2]\text{CH}_2\}$ (**1a**) (0.32 g, 2.85 mmol) was treated with 1.12 g (2.59 mmol) of $\text{Cp}^*_2\text{ZrCl}_2$ ($\text{Cp}^* = \text{C}_5\text{Me}_5$) in essentially the same manner as described for **2a**. Recrystallization from pentane gave **2b** as colorless crystals in 88% yield (1.05 g), dec $140\text{--}145^\circ\text{C}$.

(27) Manriquez, J. M.; McAlister, D. R.; Rosenberg, E.; Shiller, A. M.; Williamson, K. L.; Chan, S. I.; Bercaw, J. E. *J. Am. Chem. Soc.* **1978**, *100*, 3078.

(28) (a) Sheldrick, G. M. University of Göttingen. Sheldrick, G. M.; Krüger, C.; Goddard, R. *SHELXS-86*; Oxford University Press: Oxford, 1985; pp 175–189. (b) Sheldrick, G. M. *SHELXTL PC*, version 5.03; Siemens Analytical X-ray Instruments Inc.: Madison, WI, 1990. Refinement: Sheldrick, G. M. *SHELXL-93*; Universität Göttingen, 1993.

Table 1. Crystallographic Data for Cp₂ZrCH₂N(Me)CH₂N(Me)CH₂ (2a), Cp*₂ZrCH₂N(Me)CH₂N(Me)CH₂ (2b), and Cp*₂Zr[N(CMe₃)CCH₂N(Me)CH₂N(Me)CH₂] (3a)

	2a	2b	3a
formula	C ₁₅ H ₂₂ N ₂ Zr	C ₂₅ H ₄₂ N ₂ Zr	C ₃₀ H ₅₁ N ₃ Zr
fw	321.57	461.83	544.96
temp, K	199(2)	199(2)	199(2)
cryst size, mm	0.55 × 0.26 × 0.12	0.10 × 0.35 × 0.40	0.10 × 0.35 × 0.35
cryst syst	monoclinic	triclinic	monoclinic
space group	<i>P</i> 2 ₁ / <i>n</i>	<i>P</i> 1	<i>P</i> 2 ₁ / <i>n</i>
<i>a</i> , Å	13.858(2)	8.587(1)	10.743(1)
<i>b</i> , Å	8.292(1)	9.362(1)	19.556(2)
<i>c</i> , Å	12.856(1)	15.539(1)	13.716(1)
α, deg	90	89.80(1)	90
β, deg	105.80(1)	92.90(1)	91.16(1)
γ, deg	90	107.15(1)	90
<i>V</i> , Å ³	1421.5(3)	1192.0(2)	2881.5.0(5)
<i>Z</i>	4	2	4
cryst color, habit	colorless block	colorless block	yellow needles
<i>D</i> (calc), g cm ⁻³	1.503	1.287	1.256
μ(Mo Kα), mm ⁻¹	0.758	0.474	0.403
<i>F</i> (000)	704	492	1168
θ range, deg	3.0–27.0	3.0–26.0	3.0–26.0
limiting indices	−11 ≤ <i>h</i> ≤ 11, 0 ≤ <i>k</i> ≤ 19, 0 ≤ <i>l</i> ≤ 14	−10 ≤ <i>h</i> ≤ 10, −11 ≤ <i>k</i> ≤ 11, 0 ≤ <i>l</i> ≤ 19	−13 ≤ <i>h</i> ≤ 10, −23 ≤ <i>k</i> ≤ 22, −16 ≤ <i>l</i> ≤ 16
reflms coll	3128	4657	8263
indep reflms	3066	4655	5484
ρ _{max} , ρ _{min} , e Å ⁻³	0.776, −0.969	1.802, −1.461	0.378, −0.341
goodness-of fit on <i>F</i> ²	1.049	1.312	1.049

CI-MS [*m/e* (%): 459 (38), [M⁺ − H]; 434 (23), [M⁺ − C₂H₂]; 417 (61), [M⁺ − CH₂NCH₃]; 402 (99), [M⁺ − CH₂NMe₂]; 360 (100), [Cp*₂Zr]⁺. ¹H NMR (C₆D₆, 25 °C, 270.05 MHz): δ 1.64 (s, 4 H, NCH₂Zr), 1.86 (s, 30 H, 2 Cp*), 2.37 (s, 6 H, NCH₃), 2.48 (s, 2 H, NCH₂N). {¹H}¹³C NMR (C₆D₆, 25 °C, 67.94 MHz): δ 12.2 (s, C₅(CH₃)₅), 48.6 (s, NCH₃), 66.8 (s, NCH₂Zr), 85.3 (s, NCH₂N), 114.8 (s, C₅(CH₃)₅). Anal. Calcd for C₂₅H₄₂N₂Zr: C, 65.02; H, 9.71; N, 6.07; Zr, 19.75. Found: C, 64.62; H, 9.43; N, 5.87; Zr, 19.74.

Preparation of Cp₂ZrCH₂N(*i*-Pr)CH₂N(*i*-Pr)CH₂ (2c). Bis(lithiomethyl(isopropylamino))methane {[LiCH₂N(*i*-Pr)]₂-CH₂} (**1b**) (0.85 g, 5.05 mmol) was treated with 1.48 g (5.06 mmol) of Cp₂ZrCl₂ in essentially the same manner as described for **2a**. Recrystallization from pentane gave **2c** as colorless crystals in 73% yield (1.39 g), dec 139–142 °C. CI-MS [*m/e* (%): 376 (37), [M]⁺; 311 (33), [M⁺ − Cp]; 305 (65), [M⁺ − CH₂N(CHMe₂)]; 290 (28), [M⁺ − CH₂N(CHMe₂)(Me)]; 262 (100), [305 − CH₂NMe]; 220 (43), [Cp₂Zr]⁺; 155 (96), [CpZr]⁺. ¹H NMR (C₆D₆, 25 °C, 399.65 MHz): δ 0.85 (d, ³*J* = 6.6 Hz, 6 H, CH(CH₃)₂), 0.93 (d, ³*J* = 6.6 Hz, 6 H, CH(CH₃)₂), 1.60 (d, 2 H, NCH₂Zr), 1.91 (d, 2 H, NCH₂Zr), 2.22 (sept, ³*J* = 6.6 Hz, 2 H, CH(CH₃)₂), 2.58 (s, 2 H, NCH₂N), 1.86 (s, 10 H, 2 C₅H₅). ¹³C NMR (C₆D₆, 25 °C, 67.94 MHz): δ 18.3 (q, ¹*J* = 125.5 Hz, CH-(CH₃)₂), 20.8 (q, ¹*J* = 125.5 Hz, CH(CH₃)₂), 51.3 (t, ¹*J* = 138.0 Hz, NCH₂Zr), 55.8 (d, ¹*J* = 139.0, CH(CH₃)₂), 63.0 (t, ¹*J* = 142.2 Hz, NCH₂N), 104.1 (d, ¹*J* = 169.1 Hz, C₅H₅). Anal. Calcd for C₁₉H₃₀N₂Zr: C, 60.42; H, 8.01; N, 7.42; Zr, 24.15. Found C, 60.09; H, 7.93; N, 7.34; Zr, 24.25.

Preparation of Cp*₂ZrCH₂N(*i*-Pr)CH₂N(*i*-Pr)CH₂ (2d). Bis(lithiomethyl(isopropylamino))methane {[LiCH₂N(Me)]₂-CH₂} (**1b**) (1.27 g, 7.50 mmol) was treated with 2.94 g (6.80 mmol) of Cp*₂ZrCl₂ in essentially the same manner as described for **2a**. Removal of volatiles left red, crystalline plates of **2d** in 79% yield (2.79 g), dec 153–155 °C. CI-MS [*m/e* (%): 515 (9), [M⁺ − 1]; 445 (58), [M⁺ − CH₂N(*i*-Pr)]; 432 (100), [M⁺ − (CH₂)₂NMe₂]; 381 (26), [M⁺ − Cp*]; 360 (47), [Cp*₂Zr]⁺. ¹H NMR (C₆D₆, 25 °C, 399.65 MHz): δ 1.07 (s, 4 H, NCH₂Zr), 1.14 (d, ³*J* = 6.6 Hz, 12 H, CH(CH₃)₂), 1.86 (s, 30 H, C₅(CH₃)₅), 2.62 (s, 2 H, NCH₂N), 2.79 (sept, ³*J* = 6.6, 2 H, CH(CH₃)₂). {¹H}¹³C NMR (C₆D₆, 25 °C, 100.40 MHz): δ 11.6 (s, C₅(CH₃)₅), 19.0 (s, CH(CH₃)₂), 59.2 (s, ZrCH₂N), 68.5 (s, CH-

(CH₃)₂), 71.6 (s, NCH₂N), 117.6 (s, C₅(CH₃)₅). Anal. Calcd for C₂₉H₅₀N₂Zr: C, 67.25; H, 9.73; N, 5.41; Zr, 17.61. Found: C, 66.98; H, 9.68; N, 5.28; Zr, 17.49.

Preparation of Cp*₂Zr[N(CMe₃)CCH₂N(Me)CH₂N(Me)-

CH₂] (**3a**). The zirconium complex **2b** (0.62 g, 1.34 mmol) was dissolved in 30 mL of toluene, and the solution was cooled to −78 °C. Under stirring, 0.19 mL (1.58 mmol) of *t*-BuNC in 10 mL of toluene was added within 10 min at −78 °C. Stirring was continued for 2 h while warming to room temperature. The yellow solution that resulted was maintained at 20 °C for 16 h. During this time, the color of the solution changed to dark red. The solvent was removed under vacuum, and pentane was added to the solid residue. After filtration the solvent was reduced in vacuo to yield an orange liquid, which was cooled to −30 °C to produce yellow crystals of **3a** suitable for X-ray analysis (0.68 g, 93), dec 130–135 °C. CI-MS [*m/e* (%): 543 (26), [M]⁺; 500 (4), [M⁺ − CH₂NMe]; 487 (100), [M⁺ − CH₂CMe₂]; 459 (24), [M⁺ − *t*-BuNHC]; 443 (34), [M⁺ − CH₂N(Me)₂CH₂]; 417 (39), [M⁺ − *t*-BuNCCH₂NMe]; 360 (18), [Cp*₂Zr]⁺. IR (Nujol) ν_s(C=N): 1618 cm⁻¹. ¹H NMR (C₆D₆, 25 °C, 270.05 MHz): δ 1.27 (s, 9 H, (CH₃)₃C), 1.86 (s, 30 H, C₅(CH₃)₅), 1.95 (s, 2 H, NCH₂Zr), 2.49 (s, 3 H, NCH₃), 2.92 (s, 3 H, NCH₃), 3.32 (s, 2 H, NCH₂CN), 3.53 (s, 2 H, NCH₂N). ¹³C NMR (C₆D₆, 25 °C, 67.94 MHz): δ 12.2 (q, ¹*J* = 125.5 Hz, C₅-(CH₃)₅), 31.3 (q, ¹*J* = 126.0, (CH₃)₃C), 46.1 (q, ¹*J* = 129.2 Hz, NCH₃), 50.7 (q, ¹*J* = 132.8 Hz, NCH₃), 60.3 (m, (CH₃)₃C), 62.4 (t, ¹*J* = 125.5 Hz, NCH₂CN), 67.9 (t, ¹*J* = 124.0, ZrCH₂N), 81.4 (t, ¹*J* = 138.2 Hz, NCH₂N), 116.3 (m, C₅(CH₃)₅), 240.0 (m, NCH₂CN-*t*-Bu).

Preparation of Cp*₂Zr[N(CMe₃)CCH₂N(*i*-Pr)CH₂N(*i*-

Pr)CH₂] (**3b**). The reaction procedure and workup of the reaction were the same as described for the synthesis of **3a**: 0.32 g (0.62 mmol) of **2d** and 0.06 mL (0.68 mmol) of *t*-BuNC were used. **3b** was obtained as a colorless solid in 87% yield (0.32 g), dec 147–149 °C. CI-MS [*m/e* (%): 598 (19), [M⁺ − H]; 528 (56), [M⁺ − CH₂N(*i*-Pr)]; 543 (78), [M⁺ − CH₂CMe₂]; 514 (43), [M⁺ − CH₂N(*i*-Pr)CH₂]; 445 (36), [M⁺ − *t*-BuNCCH₂N(*i*-Pr)]; 360 (100), [Cp*₂Zr]⁺. ¹H NMR (toluene-*d*₈, 25

°C, 270.05 MHz): δ 1.06 (d, 6 H, $^3J = 6.4$ Hz, CH(CH₃)₂), 1.36 (s, 9 H, C(CH₃)₃), 1.39 (d, 6 H, $^3J = 6.4$ Hz, CH(CH₃)₂), 1.84 (s, 30 H, C₅(CH₃)₅), 1.85 (s, 2 H, NCH₂Zr), 3.17 (sept, 1 H, $^3J = 6.4$ Hz, CH(CH₃)₂), 3.25 (sept, 1 H, $^3J = 6.4$ Hz, CH(CH₃)₂), 3.51 (s, 2 H, NCH₂CN), 3.61 (s, 2 H, NCH₂N). ¹³C NMR (toluene-*d*₈, 25 °C, 100.50 MHz): δ 12.8 (q, $^1J = 125.7$ Hz, C₅-(CH₃)₅), 19.2 (q, $^1J = 126.9$ Hz, CH(CH₃)₂), 22.0 (q, $^1J = 126.9$ Hz, CH(CH₃)₂), 32.0 (q, $^1J = 128.2$ Hz, C(CH₃)₃), 50.4 (t, $^1J = 131.2$ Hz, ZrCH₂N), 53.3 (d, $^1J = 133.7$ Hz, CH(CH₃)₂), 55.6 (t, $^1J = 121.8$ Hz, NCH₂CN), 59.1 (d, $^1J = 131.2$ Hz, CH(CH₃)₂), 60.7 (m, C(CH₃)₃), 75.4 (t, $^1J = 132.8$ Hz, NCH₂N), 115.9 (m, C₅(CH₃)₅), 239.7 (s, CN \dot{t} -Bu).

Preparation of Cp*₂Zr[N(Me)CCH₂N(Me)CH₂N(Me)CH₂]

(3c). The reaction procedure and workup of the reaction were the same as described for the synthesis of **3a**: 0.88 g (1.90 mmol) of **2b** and 0.08 mL (2.48 mmol) of MeNC were used. **3c** was obtained as a colorless solid in 91% yield (0.87 g), dec 129–131 °C. CI-MS [*m/e* (%): 501 (81), [M]⁺; 458 (7), [M⁺ – CH₂-NMe]; 415 (23), [M⁺ – 2 CH₂NMe]; 360 (40), [Cp*₂Zr]⁺; 136 (100), [Cp*H]⁺. IR (Nujol) ν_s (C=N): 1625 cm⁻¹. ¹H NMR (C₆D₆, 25 °C, 399.65 MHz): δ 1.77 (s, 30 H, C₅(CH₃)₅), 1.89 (s, 2 H, NCH₂Zr), 2.44 (s, 3 H, NCH₃), 2.87 (s, 3 H, NCH₃), 2.87 (s, 3 H, CNCH₃) 3.21 (s, 2 H, NCH₂CN), 3.44 (s, 2 H, NCH₂N). {¹H}¹³C NMR (C₆D₆, 25 °C, 67.94 MHz): δ 11.4 (s, C₅(CH₃)₅), 36.3 (s, CNCH₃), 45.2 (s, NCH₃), 51.9 (s, NCH₃), 60.1 (s, NCH₂-CN), 68.2 (s, NCH₂Zr), 82.8 (s, NCH₂N), 114.6 (s, C₅(CH₃)₅), 238.8 (s, NCH₂CNMe).

Preparation of Cp*₂Zr(H)[OC=CHN(Me)CH₂N(Me)CH₂] (**4a**). The stirred solution of 0.34 g (0.74 mmol) of **2b** in 40 mL of toluene at 20 °C was treated with purified carbon monoxide (specif. N4.7) at atmospheric pressure. A fast uptake of CO was indicated by a color change of the solution from light yellow to red. After 2 h toluene was replaced by pentane. After filtration the solvent was evaporated to produce a yellow noncrystalline solid characterized as **4a** (0.34 g, 95% yield). CI-MS [*m/e* (%): 488 (21), [M]⁺; 445 (7), [M⁺ – CH₂NMe]; 415

(23), [M⁺ – 2 CH₂CMe]; 360 (40), [Cp*₂Zr]⁺; 136 (100), [Cp*H]⁺. ¹H NMR (C₆D₆, 25 °C, 270.05 MHz): δ 1.95 (s, 30 H, C₅(CH₃)₅), 2.30 (s, 3 H, NCH₃), 2.45 (s, 3 H, NCH₃), 2.97 (d, $^4J = 1.2$ Hz, 2 H, NCH₂CO) 3.31 (s, 2 H, NCH₂N), 5.53 (t, $^4J = 1.2$ Hz, 1 H, OCCHN), 5.95 (s, 1 H, ZrH). {¹H}¹³C NMR (C₆D₆, 25 °C, 67.94 MHz): δ 11.7 (s, C₅(CH₃)₅), 42.2 (s, NCH₃), 42.3 (s, NCH₃), 58.4 (s, CH₂CO), 74.1 (s, NCH₂N), 116.2 (s, OCCH), 118.1 (s, C₅-(CH₃)₅), 142.6 (s, OCCH).

Preparation of Cp*₂Zr(H)[OC=CHN(*i*-Pr)CH₂N(*i*-Pr)-

CH₂] (**4b**). The reaction procedure and workup of the reaction was the same as described for the synthesis of **4a**: 0.54 g (1.04 mmol) of **2d** was used. After the solvent was evaporated, an orange noncrystalline solid, **4b** (0.49 g, 87% yield), was obtained. CI-MS [*m/e* (%): 543 (100), [M⁺ – H]; 472 (22), [M⁺ – CH₂N(*i*-Pr)]; 360 (6), [Cp*₂Zr]⁺; 136 (56), [Cp*H]⁺. ¹H NMR (C₆D₆, 25 °C, 270.05 MHz): δ 1.02 (d, $^3J = 6.4$ Hz, 6 H CH-(CH₃)₂), 1.17 (d, $^3J = 6.4$ Hz, 6 H, CH(CH₃)₂), 1.97 (s, 30 H, C₅(CH₃)₅), 2.65 (sept, $^3J = 6.4$ Hz, 1 H, CH(CH₃)₂), 3.04 (sept, $^3J = 6.4$ Hz, 1 H, CH(CH₃)₂), 3.09 (s, 2 H, NCH₂CO) 3.64 (s, 2 H, NCH₂N), 5.51 (s, 1 H, OCCHN), 5.98 (s, 1 H, ZrH). {¹H}¹³C NMR (C₆D₆, 25 °C, 67.94 MHz): δ 11.8 (s, C₅(CH₃)₅), 19.9 (s, CH(CH₃)₂), 21.2 (s, CH(CH₃)₂), 51.7 (s, CH₂CO), 52.7 (s, CH-(CH₃)₂), 53.6 (s, CH(CH₃)₂), 65.6 (s, NCH₂N), 111.6 (s, OCCH), 119.5 (s, C₅(CH₃)₅), 144.4 (s, OCCH).

Acknowledgment. We thank the Fonds der Chemischen Industrie and the Volkswagenstiftung for financial support.

Supporting Information Available: Text giving tables of atomic coordinates and isotropic thermal parameters, complete bond lengths, and thermal parameters for **2a**, **2b**, and **3a** (21 pages). Ordering information is given on any current masthead page.

OM980470Q